Electronic Supplementary Information for the manuscript:

Supramolecular Interactions Impacting on the Water Stability of Tubular Metal-Organic Frameworks

Marco Taddei,[a] Andrea Ienco,*[b] Ferdinando Costantino*[a,b] and Annalisa Guerri[c]

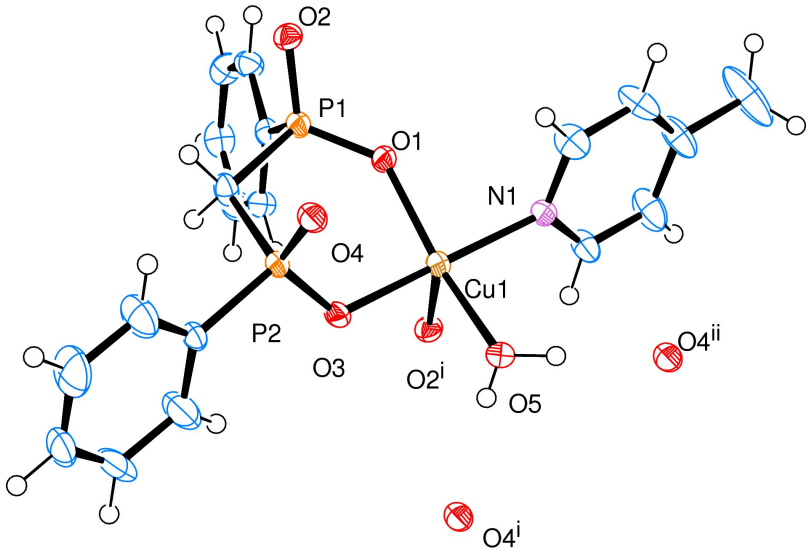

Figure 1S: Perspective view of the asymmetric unit of $[[Cu_2(H_2O)_2(pcp)_2bpye]_n$. For sake of clarity, the Oxygen atoms involved in the hydrogen bonds with the water molecule and in the Copper coordination are also reported. ORTEP drawing with 50% probability ellipsoid. O2i and O4i have been obtained using x+1,y,z symmetry transformation and O4ii has been obtained using -x+1,-y,-z symmetry transformation.

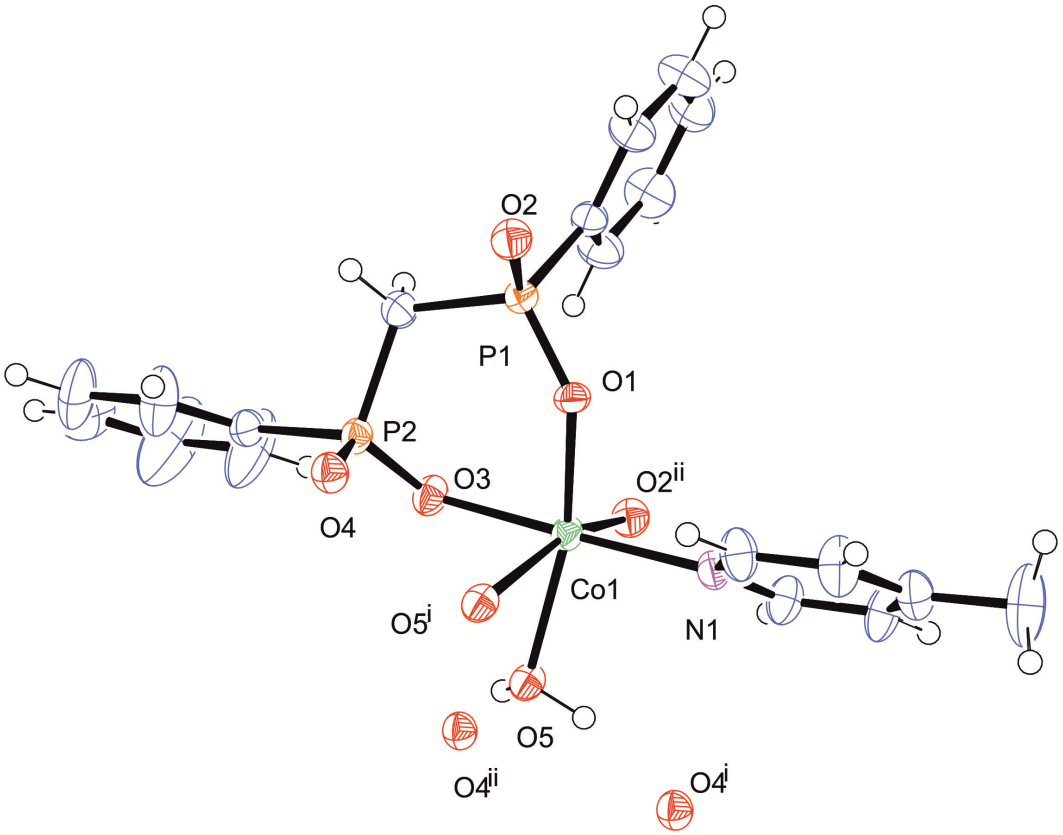

Figure 2S: Perspective view of the asymmetric unit of $[[Co_2(H_2O)_2(pcp)_2bpye]_n$. For sake of clarity, the Oxygen atoms involved in the hydrogen bonds with the water molecule and in the Cobalt coordination are also reported. ORTEP drawing with 50% probability ellipsoid. $O4^i$ and $O5^i$ have been obtained using -x+1,-y,-z symmetry transformation while $O2^{ii}$ and $O4^{ii}$ have been obtained using x+1,y,z symmetry transformation.

	STRIP	**Co-pcp-bpye**
Empirical formula	C19 H20 Cu N O5 P2	C19 H20 Co N O5 P2
Formula weight	467.84	463.23
Temperature	173(2) K	293(2) K
Wavelength	1.5418 Å	0.71069 Å
Crystal system	Triclinic	Triclinic
Space group	P -1	P -1
Unit cell dimensions	a = 5.6921(2) Å	a = 5.7631(3) Å
	b = 13.3051(5) Å	b = 13.0859(8) Å
	c = 13.9862(6) Å	c = 13.6759(7) Å
	α= 64.365(4)°.	α= 67.345(5)°.
	β= 80.711(3)°.	β= 81.812(5)°.
	γ = 86.393(3)°.	γ = 89.757(5)°.
Volume	942.42(7) $Å^3$	940.64(10) $Å^3$
Z	2	2
Density (calculated)	1.649 Mg/m^3	1.635 Mg/m^3
Absorption coefficient	3.532 mm^{-1}	1.115 mm^{-1}
F(000)	480	476
Crystal size	0.15 x 0.12 x 0.08 mm^3	0.2 x 0.1 x 0.04 mm^3
Theta range for data collection	3.865 to 72.375°.	3.881 to 28.876°.
Index ranges	-6<=h<=6, -16<=k<=16, -17<=l<=17	-7<=h<=7, -17<=k<=15, -17<=l<=18
Reflections collected	17585	7559
Independent reflections	3666 [R(int) = 0.0513]	4188 [R(int) = 0.0416]
Completeness to theta =	(67.68°) 99.8 %	(25.00°) 99.4 %
Absorption correction	Semi-empirical from equivalents	Semi-empirical from equivalents
Max. and min. transmission	0.838 and 0.393	1 and 0.76057
Refinement method	Full-matrix least-squares on F^2	Full-matrix least-squares on F^2
Data / restraints / parameters	3666 / 0 / 261	4188 / 2 / 259
Goodness-of-fit on F^2	1.004	0.84
Final R indices [I>2sigma(I)]	R1 = 0.0365, wR2 = 0.0875	R1 = 0.042, wR2 = 0.0676
R indices (all data)	R1 = 0.0626, wR2 = 0.0983	R1 = 0.0891, wR2 = 0.0746
Largest diff. peak and hole	0.445 and -0.385 $e.Å^{-3}$	0.381 and -0.429 $e.Å^{-3}$

Table 1S. Crystal data and structure refinement for STRIP and Co-pcp-bpye

STRIP		Co-pcp-bpye	
Cu(1)-O(1)	1.964(2)	Co(1)-O(1)	2.059(2)
Cu(1)-O(2)#1	2.207(2)	Co(1)-O(2)#1	2.0690(19)
Cu(1)-O(3)	1.963(2)	Co(1)-O(3)	2.0805(18)
Cu(1)-O(5)	1.985(2)	Co(1)-O(5)	2.116(2)
		Co(1)-O(5)#2	2.420(2)
Cu(1)-N(1)	2.023(2)	Co(1)-N(1)	2.163(2)
P(1)-O(1)	1.518(2)	P(1)-O(1)	1.510(2)
P(1)-O(2)	1.501(2)	P(1)-O(2)	1.503(2)
P(1)-C(1)	1.829(3)	P(1)-C(1)	1.823(3)
P(1)-C(11)	1.808(3)	P(1)-C(11)	1.804(3)
P(2)-O(3)	1.516(2)	P(2)-O(3)	1.503(2)
P(2)-O(4)	1.508(2)	P(2)-O(4)	1.510(2)
P(2)-C(1)	1.813(3)	P(2)-C(1)	1.803(3)
P(2)-C(21)	1.803(3)	P(2)-C(21)	1.805(3)
O(1)-Cu(1)-O(2)#1	105.74(8)	O(1)-Co(1)-O(2)#1	108.90(8)
O(1)-Cu(1)-O(3)	92.38(9)	O(1)-Co(1)-O(3)	88.75(8)
O(1)-Cu(1)-O(5)	159.86(10)	O(1)-Co(1)-O(5)	157.26(8)
O(1)-Cu(1)-N(1)	88.77(10)	O(1)-Co(1)-O(5)#2	87.66(8)
O(2)#1-Cu(1)-O(3)	94.21(9)	O(1)-Co(1)-N(1)	89.22(9)
O(2)#1-Cu(1)- O(5)	94.40(9)	O(2)#1-Co(1)-O(3)	92.35(7)
O(2)#1-Cu(1)- N(1)	90.92(10)	O(2)#1-Co(1)-O(5)	93.63(8)
O(3)-Cu(1)-O(5)	86.57(10)	O(2)#1-Co(1)-N(1)	88.93(8)
O(3)-Cu(1)-N(1)	174.22(10)	O(2)#1-Co(1)-O(5)#2	163.43(8)
O(5)-Cu(1)-N(1)	90.39(11)	O(3)-Co(1)-O(5)	87.25(8)
		O(3)-Co(1)-O(5)#2	87.31(7)
		O(3)-Co(1)-N(1)	177.86(10)
		O(5)-Co(1)-N(1)	94.38(9)
		O(5)-Co(1)-O(5)#2	69.81(9)
		O(5)#2-Co(1)- N(1)	91.95(8)

Table 2S. Selected bond lengths [Å] and angles [°] for STRIP and Co-pcp-bpye.
Symmetry transformations used to generate equivalent atoms: #1 x+1,y,z; #2 -x+1,-y,-z.

D-H...A	d(D-H)	d(H...A)	d(D...A)	<(DHA)
$[[Cu_2(H_2O)_2(pcp)_2bpye]_n$				
O(5)-H(5A)...O(4)#1	0.96(4)	1.76(5)	2.682(3)	162(4)
O(5)-H(5B)...O(4)#2	0.72(4)	1.97(4)	2.696(3)	174(5)
$[[Co_2(H_2O)_2(pcp)_2bpye]_n$				
O(5)-H(5A)...O(4)#1	0.907(17)	1.792(19)	2.662(3)	160(3)
O(5)-H(5B)...O(4)#2	0.845(16)	1.850 (18)	2.686(3)	170(3)

Table 3S. Hydrogen bonds for STRIP and Co-pcp-bpye. Symmetry transformations used to generate equivalent atoms: #1 -x+1, -y, -z; #2 x+1, y, z.

Rietveld quantitative phase analysis

The Bish and Howard formula (eq.1)

$$W_m = \frac{a_m S_m}{\sum_{k=1}^{k=m} a_k S_k}$$

has been used for the calculation of the relative weight fraction of the MONT2 and STRIP phases for the powdered samples collected at different days.

W_m and a_k are the weight fraction of the mth component in the sample and its calculated density, respectively; a_k is given as follows: $a_k = Z_k M_k U_k$ where Z_k, M_k, and U_k are the number of chemical formula units in a unit cell, the molecular weight, and the unit-cell volume, respectively.

The structural data for the MONT2 and STRIP phases were taken from single crystal data. The unit cell parameters of MONT2 phase were also refined as the original crystallographic data were collected at 100 K and the XRPD patterns at room temperature.

Sample	**1 (1d)**	**2 (2d)**	**3 (4d)**	**4 (8d)**	**5 (22d)**
pattern range, 2θ/deg	4-60	4-60	4-60	4-60	4-60
Step; Time/step					
Rp	0.042	0.041	0.028	0.047	0.035
Rwp	0.057	0.053	0.039	0.062	0.046
$R_F 2$	0.094	0.091	0.21	0.107	0.156
GOF	1.59	1.36	0.8	1.24	1.21
Wt fraction of the two phases (%)	MONT: 93.16(3) STRIP: 6.8(2)	MONT :83.02(6) STRIP: 16.9(2)	MONT: 69.1(2) STRIP: 30.8(5)	MONT : 55.3(2) STRIP : 44.6(3)	MONT : 25.7(2) STRIP: 74.2(1)

Table 4S. Details of the Rietveld refinement and quantitative phase analysis for samples **1÷5**

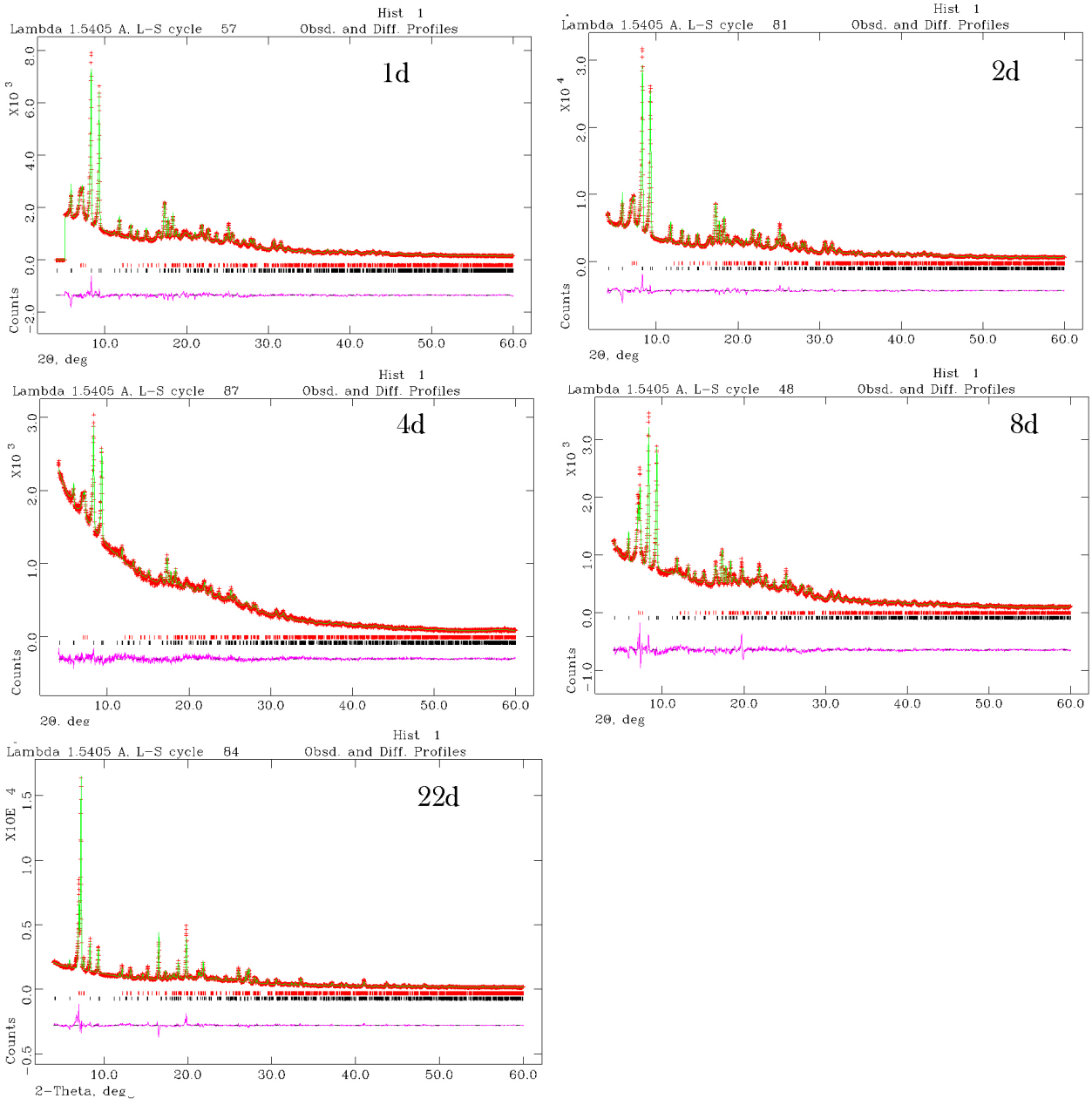

Figure 3S. Rietveld plots for MONT2 collected at different days.

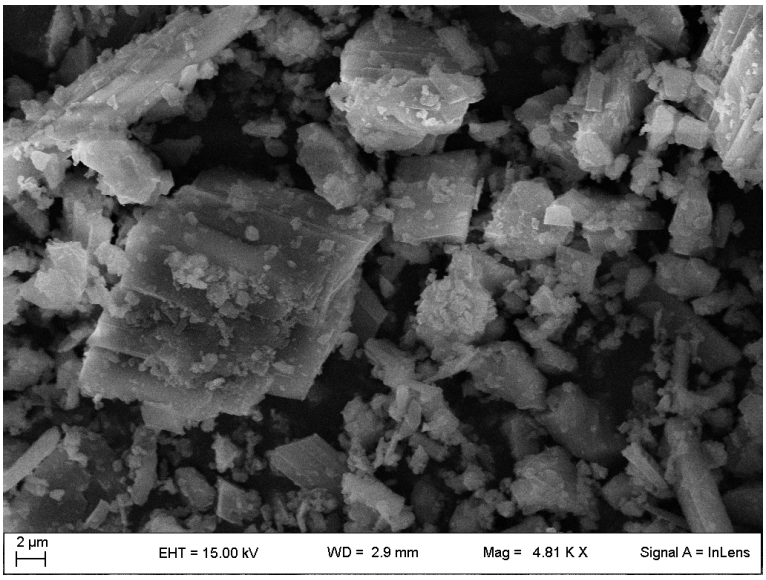

Figure 4S. SEM image of the pure STRIP phase.

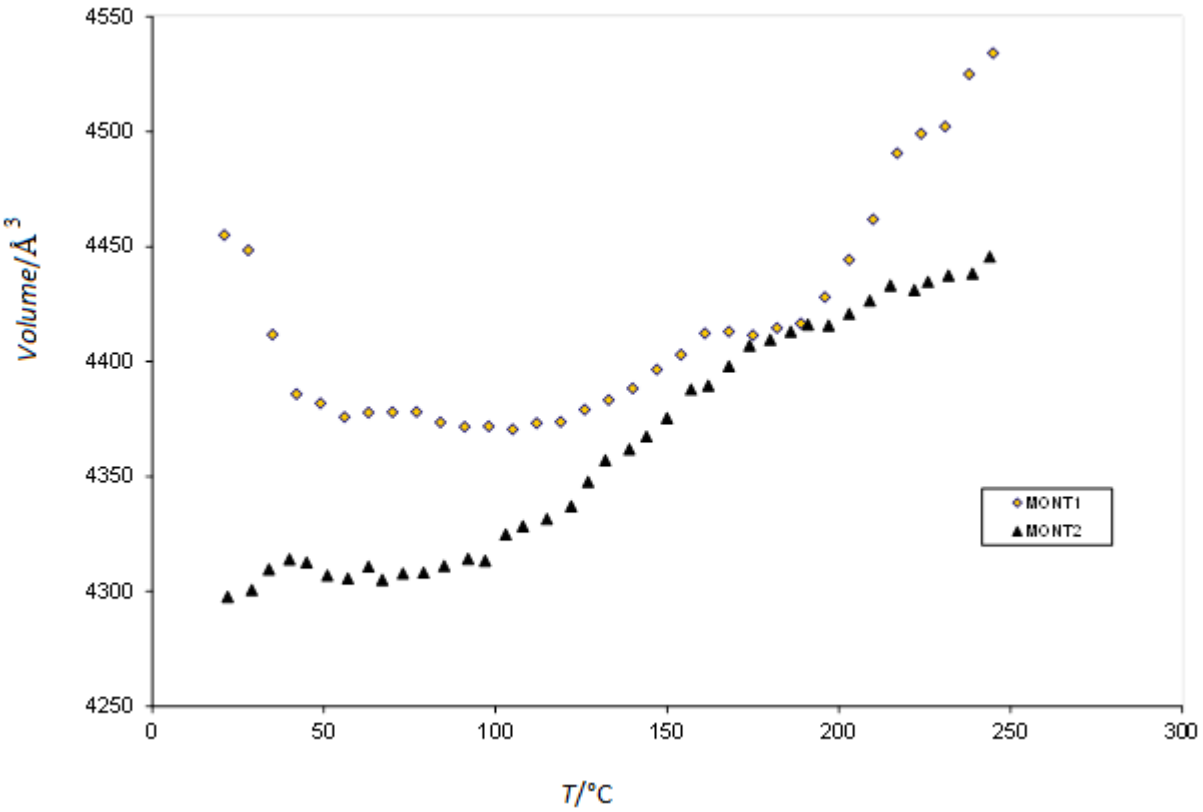

Figure 5S. Change of the cell volume divided by the number of tube in the unit cell for **MONT1** and **MONT2** as function of the temperature using qualitative temperature-dependent X-ray diffraction (TDXD). The TDXD was performed under flowing air with a powder diffractometer equipped with a curved position-sensitive detector (INEL CPS 120) and a high temperature attachment from Rigaku. The detector was used in a semifocusing arrangement by reflection (Cu $K_{\alpha 1}$ radiation). With this geometry, the stationary sample is deposited on a flat sample holder located at the center of the goniometer. The counting time was 45 min for each diffraction pattern. Decompositions were carried out in flowing air with a heating rate of 10 °C h-1 between 17 and 600 °C. (Temperature calibration was carried out with standard materials in the involved

temperature range). The cell parameters of the heated samples were determined by performing a LeBail refinement, using the program FULLPROF, of selected thermal diffraction patterns.
This analysis also revealed a reversible dilatation of the tubular frameworks (Figure 5S). In fact the cell volume of 1 increases slowly up to 100°. A brusque change is then observed around 110 °C, followed by a slower increase after 200°C. Additional cooling and heating experiments, carried out three times from room temperature up to 200 °C, showed a good reproducibility of this variation. The same experiment on **MONT2** shows a shrinking of the volume due to the escaping of the solvent water molecules, followed by a progressive increasing of the cell volume up to 300 °C.